Terbit *online* pada laman web jurnal : https://jes-tm.org/index.php/jestm/index

Journal of Engineering Science and Technology Management

| ISSN (Online) 2828 -7886 |

Article

Dynamic Modeling and Nyquist Stability Analysis of a Non-Interacting Two-Tank Series Thermal System

Yogi Yolanda[1] Yola Bertilsya Hendri[2], Salma Liska[3], Lisa Legawati[4], Suhendri[5], Alltop Amri Ya Habib[6], Zulfansyah[7]

[1,2,3,4,5,6,7]Department of Chemical Engineering, Faculty of Engineering, Universitas Riau, Pekanbaru, Indonesia

DOI: 10.31004/jestm.v6i2.431

E-mail: *yogi.yolanda@lecturer.unri.ac.id

ARTICLE INFORMATION

Volume 6 Issue 2
Received: 02 March 2026
Accepted: 05 June 2026
Publish *Online*:14 June 2026
Online: at https:JESTM.org/

Keywords

Two-tank series system
Nyquist plot
Dynamic modeling
Process control
System stability

A B S T R A C T

Series tank systems are vital in chemical industries but susceptible to mass and thermal disturbances, making stability analysis essential. This study models the level and temperature dynamics of a non-interacting two-tank system equipped with a heater in Tank-01, analyzing its stability via Nyquist plots. The methodology involves laboratory step-response experiments validated against mathematical models derived using Laplace Transforms and Explicit Euler methods. Results demonstrate the models closely match experimental data with high determination coefficients (R^2 up to 0.995). Error analysis yields a minimum Root Mean Square Error (RMSE) of 0.061 °C and a Mean Absolute Percentage Error (MAPE) as low as 0.18%, confirming high predictive accuracy. Physically, Tank-01 exhibits first-order characteristics, while Tank-02 functions as a second-order system. The physical system successfully handled +52% and -35% step disturbances within liquid height limits of 3–24 cm and feed flow rates of 40.33–136.5 cm^3/s. Furthermore, Nyquist analysis confirms the thermal process is open-loop stable across all tested capacities. Maximum level and thermal process gains were 0.3787 and 0.0062, respectively. Ultimately, this study confirms the non-interacting two-tank system possesses stable, self-regulating open-loop characteristics against load disturbances within operational limits.

1. Introduction

The series tank system is a fundamental and commonly encountered unit operation in the chemical process industry, both as a temporary storage unit and as a stirred tank reactor (CSTR) (Akkoç, 2025; Ballesteros-Moncada et al., 2015). In its application, this system often faces challenges in the form of complex dynamic interactions, where load disturbances such as changes in mass flow rate and thermal fluctuations can propagate between operating units. The inability of the system to dampen these disturbances can cause process instability, which can lead to a decline in product quality and occupational safety risks (Wang et al., 2024). Therefore, a thorough understanding of process dynamics and system stability limits is an absolute prerequisite before controller design is carried out.

Previous studies have attempted to model the dynamics of level and temperature in tank systems. Hermawan et al. (2016) conducted dynamic simulations and level control designs on pure capacitive systems, as well as analyzing non-interacting tank configurations (Hermawan et al., 2010, 2016). Research continues to evolve towards intelligent and adaptive systems. For example, Suryatini et al. (2024) recently developed an IoT and PLC-based level control system to monitor the response of coupled tanks in real-time (Suryatini et al., 2024). On the other hand, Tunjung et al. (2021) explored temperature control in thermal mixing processes using adaptive fuzzy PID algorithms (Tunjung et al., 2021). Although various modern control methods have been offered, the majority of these studies focus more on controller design and time domain response, but not many have explored in depth the fundamental stability limits in the frequency domain.

Frequency domain stability analysis provides insights that are not visible in the time domain, especially regarding how close the system is to unstable conditions. One robust analysis method for open-loop systems is the Nyquist criterion. The use of Nyquist plots offers visual advantages in determining stability limits and safe process gain ranges. These characteristics are crucial for predicting the system's resistance to oscillations caused by transportation lag in the flow of hot fluid between tanks, which is often overlooked in simple modeling. Based on this background, this study aims to model the level and temperature dynamics in a non-interacting series two-tank system with a heater in the first tank, and analyze its stability using Nyquist plots. This study combines a laboratory experimental approach to obtain physical parameters and mathematical model validation. The main focus is on evaluating the system's response to step disturbances in the feed flow rate and heater energy, as well as proving the stability region of the system through computationally simulated Nyquist diagrams.

Therefore, this study aims to model the level and temperature dynamics of a non-interacting two-tank series thermal system and analyze its stability using Nyquist plots. The system's behavior under various step disturbances is investigated to evaluate its self-regulating characteristics. To bridge the existing research gap, this study provides a new contribution by presenting a comprehensive multi-variable dynamic modeling that simultaneously couples liquid level and temperature dynamics in a non-interacting two-tank series system with a heater. The primary novelty lies in utilizing Nyquist stability plots to rigorously assess the open-loop thermal stability while taking into account the non-linearities and physical transport lag of the multi-capacity process. Consequently, this work establishes a clear, validated baseline for both time-domain transient responses and frequency-domain stability, which is essential for designing robust future control systems in industrial thermal processes.

2. Literature Review

2.1 Characteristics of Multicapacity Tank Systems

In industrial process operations, the flow of mass or heat through a single tank unit typically results in a first-order state equation. However, when fluid flows through two or more tanks arranged in series, the system is classified as a second-order or n-th order system (Seborg et al., 2016). Series tank systems are categorized into two primary types based on the nature of interaction between the units:

1) Non-Interacting Series Tank (NIT) System. In this configuration, the process variables in the second tank have no back-effect on the variables in the first tank (Naik & Kanagalakshmi, 2020). Changes in the first tank propagate to subsequent tanks, but the reverse does not occur.
2) Interacting Series Tank (IT) System: This system involves variables that mutually influence one another, often due to material or energy feedback (recycle streams), resulting in more complex transfer functions

Conventional modeling paradigms in process simulation for cascaded and non-interacting systems heavily depend on idealized transfer functions or exact inverse Laplace solutions (Seborg et al., 2016). Although mathematically rigorous, such traditional analytical methodologies exhibit inherent limitations when handling structural non-linearities, as they operate under the assumption of quasi-static physical properties and localized operating regions.

Conversely, implementing high-fidelity alternatives like Computational Fluid Dynamics (CFD), while spatially accurate, introduces a prohibitive computational burden that restricts their utility in real-time control design. To balance mathematical tractability with operational fidelity, this study adopts a dual-modeling verification strategy. The constraints of the analytical inversion are mitigated by running a decentralized finite-difference numerical scheme (Explicit Euler) in parallel. This methodology provides a robust platform to cross-validate dynamic trajectories while simultaneously capturing the transient non-linear artifacts of coupled mass and thermal transport lags.

2.2 Concept of Dynamic System Stability

Stability is a critical parameter in process control. A dynamic system is technically considered stable if every bounded input results in a bounded output, regardless of its initial state (Nise, 2025). In practical applications, these boundaries are determined by the physical quantities and operational capacities of the equipment. If the system response exceeds these limits or exhibits sustained oscillations, it is declared unstable.

From an industrial engineering perspective, evaluating bounded-input bounded-output (BIBO) criteria must be extended to consider asymptotic stability, wherein the system variables naturally return to their initial steady-state equilibrium after the decay of transient disturbances. In multi-stage thermal and hydraulic processes, asymptotic stability serves as a crucial determinant for both process safety and system controllability. Without a guaranteed asymptotic decay, minor fluctuations in feed flow rates or heating elements can propagate into sustained or growing oscillations. In industrial operations, such undamped behaviors elevate the risk of hazardous scenarios, including catastrophic vessel overflow or uncontrolled localized overheating, which directly compromises mechanical integrity. Furthermore, a system that exhibits high inherent stability reduces the control effort required by automated feedback loops, preventing actuator saturation and ensuring that downstream target variables remain within tight, predictable operational limits.

2.3 Frequency Response Analysis and the Nyquist Criterion

Frequency response analysis examines the behavior of a system's output relative to a sinusoidal input over a long period. The primary parameters in this analysis are the Amplitude Ratio (AR), which represents process gain, and the Phase Angle (θ), which indicates the lag or lead of the output signal relative to the input (Chen et al., 2024).

The Nyquist Plot serves as an alternative representation of frequency response information in the form of a polar plot of the transfer function $G(j\omega)$ on a complex plane. According to the Nyquist stability criterion, an open-loop system is unstable if its plot encircles the critical point (-1, j0) clockwise as the frequency ω ranges from 0 to ∞ (Ogata, 2020). This method is highly effective for visually determining stability limits compared to conventional time-domain methods.

In practical engineering interpretations, the evaluation of frequency response trajectories must quantitatively incorporate relative stability metrics, specifically gain margin (GM) and phase margin (PM). The gain margin quantifies the allowable increase in open-loop gain before the system lapses into instability, whereas the phase margin defines the additional tolerance for phase lag—such as transportation delays inherent in fluid networks—prior to the onset of oscillation. In a polar plot configuration, these criteria define the geometric proximity of the transfer function trajectory $G(j\omega)$ to the critical inversion point (-1, j0), providing a deterministic measure of robust system stability margins under parametric variations.

3. Research Methodology

This study was conducted with two preliminary experiments, the first to determine the parameters in a steady state and the second to calibrate the measuring instruments. Dynamic experiments were conducted to determine the dynamics of the level and temperature in a series of two tanks with a heater in tank 1, and a computer simulation was conducted to determine the stability of the system. The series of experimental equipment can be seen in Fig.1.

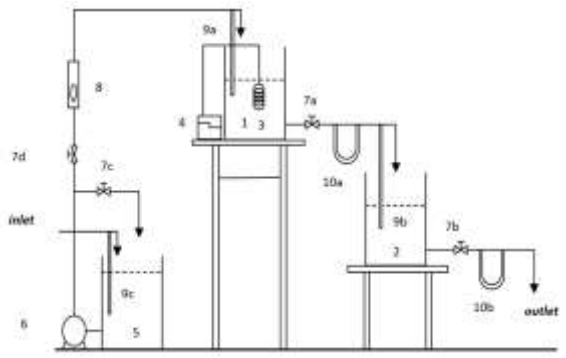

Figure. 1. Experimental equipment setup

Note:

1. Tank 1	7c. Kickback valve
2. Tank 2	7d. Tank 1 input valve
3. Heater	8. Rotameter
4. Watt regulator	9a. Tank 1 thermometer
5. Feed tank	9b. Tank 2 thermometer
6. Pump	9c. Feed tank thermometer
7a. Tank 1 output valve	10a. Orifice flowmeter 1
7b. Tank 2 output valve	10b. Orifice flowmeter 2

Before conducting the step-response experiments, all primary instruments were thoroughly calibrated to guarantee the accuracy and reproducibility of the transient data. We verified the temperature sensors via a multi-point method using ice and boiling water baselines, which secured an operational accuracy within ± 0.1 °C. The ultrasonic liquid-level transmitters were also checked against manual physical scales, showing a measurement uncertainty of only ± 0.05 cm. To avoid random experimental errors and ensure repeatability, each dynamic test run was performed in triplicate under constant ambient conditions. The resulting time-domain curves showed minimal variation (variance < 2.5%), proving that the experimental dataset is highly reliable for model validation.

3.1 Preliminary Experiment

This preliminary experiment involves calibrating measuring instruments (rotameter, manometer, and thermometer) and determining various steady-state parameters (K, τ, α, β, f_i, T_i, h_1, T_1, f_1, T_2, h_2, f_2 and q_e).

3.2 Dynamic Experiment

Dynamic experiments constitute the core of this study, aiming to evaluate the transient responses of liquid levels and temperatures in both tanks under specific disturbances.

The flowchart is presented in the following Fig.2.

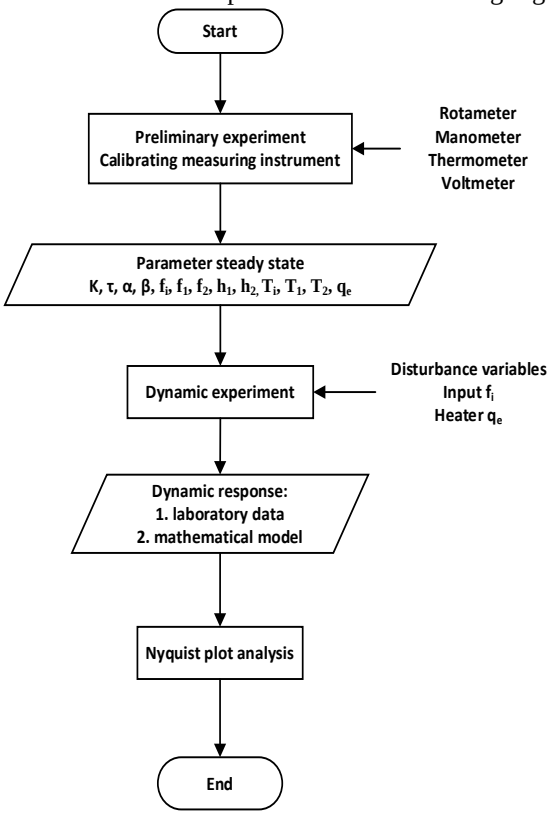

Fig. 2. Process flow diagram

In the hydraulic dynamic test, a flow disturbance was introduced by altering the feed valve opening to Tank 1. Meanwhile, the intermediate valve connecting the tanks and the outlet valve of Tank 2 were fixed at their steady-state positions. The resulting liquid level variations in both tanks were recorded at specific time intervals. For the thermal dynamic test, the feed flow rate was maintained constant at its steady-state value while a thermal disturbance was applied by heating the water in Tank 1. With all valve openings held constant, the temperature changes in both tanks were recorded periodically.

3.3 Mathematical Modeling

Mathematical modeling of temperature and level dynamics using mass balance and energy balance. Differential equations are linearized using deviation variables to obtain the Transfer Function in the Laplace domain (Borisov et al., 2020). The following assumptions were made in the modeling:

1. The density of the liquid is considered constant and does not change with temperature and time.
2. The heat capacity is considered constant and is not a function of temperature.
3. The outlet temperature of the tank is the same as the temperature inside the tank.

While these foundational assumptions simplify the mathematical tractability of the coupled differential equations, their physical implications in a non-isothermal operation warrant closer examination. Under practical conditions, temperature field variations induce localized density gradients and alter the specific heat capacity of the liquid medium. However, within the narrow operational temperature envelope examined in this study (spanning approximately 29 °C to 31 °C), the maximum theoretical variance in fluid density and heat capacity is less than 0.2%. Consequently, treating ρ and Cp as static parameters introduces a negligible truncation error while preserving the linearity required for analytical inversion. Furthermore, the assumption of perfect mixing—equating the interior tank temperature to the effluent stream—is justified by the high turnover rate and fluid turbulence maintained during the trials. This fluid state minimizes internal spatial temperature variations and prevents thermal stratification, thereby validating the lumped-parameter approach for this multi-capacity network.

1) Mass Transfer Function (Level Response)

Mass balance of Tank 1 and Tank 2 can be written:

$$\frac{dh_1(t)}{dt} = \frac{[f_i(t) - f_1(t)]}{A_1} \quad (1)$$

$$\frac{dh_2(t)}{dt} = \frac{[f_1(t) - f_2(t)]}{A_2} \quad (2)$$

The outflow rate (f_1 and f_2) depends on the square root of the liquid level:

$$f_1(t) = C_{v1}\sqrt{h_1(t)} \quad (3)$$

$$f_2(t) = C_{v2}\sqrt{h_2(t)} \quad (4)$$

where Cv_1 and Cv_2 are the valve coefficients for Tank 1 and Tank 2, respectively.

Equations (3) and (4) are linearized around their steady-state operating points using a Taylor series expansion. By expressing the equations in terms of deviation variables and transforming them into the Laplace domain, the liquid level response in Tank 2 (H_2) to changes in feed flow rate (F_i) follows second-order system dynamics. This relationship is expressed as:

$$H_2(s) = \frac{K_{p1}}{(\tau_{p1}{}^2 s^2 + 2\xi_1 \tau_{p1} s + 1)} F_i(s) \quad (5)$$

$$H_2(s) = G_L(s) F_i(s) \quad (6)$$

Where K_{p1} is the mass process gain, τ_{p1} is the process time constant, ξ_1 is the damping factor, and G_L represents the overall level transfer function of the system. The overall block diagram for the mass balance system is illustrated in Figure

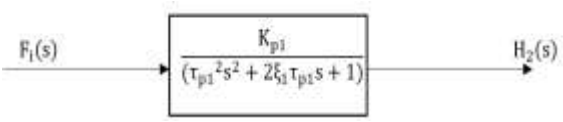

Fig. 3. Overall mass balance block diagram

2) Heat Transfer Function (Temperature Response)

Assuming perfect mixing, where the tank outlet temperature is identical to the temperature inside the tank, the energy balances for Tank 1 and Tank 2 can be written as:

$$\frac{dT_1(t)}{dt} = \frac{f_i(t)}{A_1 h_1(t)}[T_i(t) - T_1(t)] + \frac{q_e(t)}{\rho C_p A_1 h_1(t)} \quad (7)$$

$$\frac{dT_2(t)}{dt} = \frac{f_1(t)}{A_2 h_2(t)}[T_1(t) - T_2(t)] \quad (8)$$

Equations (7) and (8) are non-linear. Therefore, they are linearized around their steady-state operating points using a Taylor series expansion. By expressing the linearized equations in terms of deviation variables and transforming them into the Laplace domain, the individual effects of the input variables on the system can be analyzed. Based on the superposition principle for linear systems, the total temperature response (T_2) is the sum of the effects of the three input variables working simultaneously, which are detailed as follows:

a) The Effect of Heating as a Control Variable (q_e)

Heat input (q_e) is supplied to Tank 1. This heat energy will raise the temperature in Tank 1, causing the hot fluid to flow to Tank 2. Due to passing through two tank capacities, the temperature response T_2 to q_e experiences a delay (lag) which is described as a second-order system.

$$T_2(s) = \frac{K_{p4}}{(\tau_{p2}{}^2 s^2 + 2\xi_2 \tau_{p2} s + 1)} q_e(s) \quad (9)$$

$$T_2(s) = G_q(s) q_e(s) \quad (10)$$

b) The Effect of Feed Temperature Disturbance (T_i)

Changes in the temperature of the incoming fluid (T_i) constitute an external disturbance. If the feed temperature rises, heat will be carried into Tank 1 and then into Tank 2. This disturbance path is represented by gain Kp_3 with second order dynamics.

$$T_2(s) = \frac{K_{p3}}{(\tau_{p2}{}^2 s^2 + 2\xi_2 \tau_{p2} s + 1)} T_i(s) \quad (11)$$

$$T_2(s) = G_T(s) T_i(s) \quad (12)$$

c) The Effect of Flow Rate Disturbance (F_i)

Changes in inflow (Fi) have the most complex impact because they affect the system through two different physical pathways. Changes in flow rate alter the residence time of the liquid in the tank, which directly affects the heat balance. Changes in flow rate alter the liquid level height (H_1), which then alters the flow rate entering Tank 2, carrying its heat energy with it.

Therefore, the transfer function for flow rate disturbance (G_F) is the sum of both paths:

$$T_2(s) = \frac{K_{p2}}{(\tau_{p2}{}^2 s^2 + 2\xi_2 \tau_{p2} s + 1)} F_i(s) + \frac{K_{p5}}{(\tau_{p3}{}^2 s^2 + 2\xi_3 \tau_{p3} s + 1)} F_i(s) \quad (13)$$

$$T_2(s) = G_F(s) F_i(s) \quad (14)$$

d) Overall Model Equation

By combining the three components above, the complete mathematical equation for Tank 2 temperature is:

$$T_2(s) = G_q(s) q_e(s) + G_T(s) T_i(s) + G_F(s) F_i(s) \quad (15)$$

Where G_q, G_T, and G_F represent the overall transfer functions relating the tank temperature response to changes in the heat input, inlet temperature, and feed flow rate, respectively. Furthermore, K_{p2}, K_{p3}, K_{p4}, and K_{p5} are the thermal process gains for their respective input pathways. Similarly, τ_{p2} and τ_{p3} are the thermal process time constants, while ξ_2 and ξ_3 are the damping factors governing the dynamic behavior of the temperature responses.

The combined dynamic effects of these multiple inputs on the tank temperature are visualized

in the overall heat balance block diagram in Figure.4.

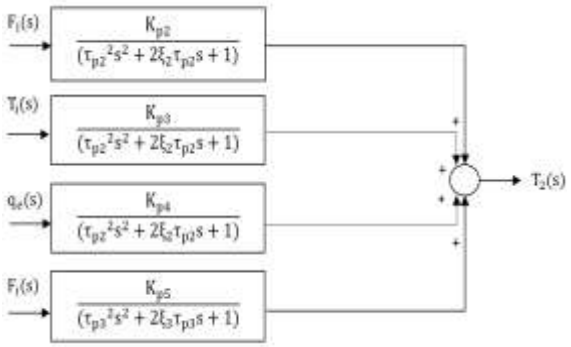

Figure. 4. Overall heat balance block diagram

4. Results and Discussion

Based on preliminary experiments under steady state conditions, physical parameters and process parameters were obtained and summarized in Table 1 and Table 2 respectively. These parameters form the basis of the coefficients in the transfer function that has been derived in the methodology.

Table 1. Steady-State Operating Conditions and Physical Parameters

Symbol	Description	Value	Unit
$\bar{f_1}$	Volumetric feed flow rate	89.73	cm^3/sec
$\bar{f_1}$	Volumetric outflow rate from Tank 1	89.73	cm^3/sec
$\bar{f_2}$	Volumetric outflow rate from Tank 2	89.73	cm^3/sec
$\overline{h_1}$	Liquid level in Tank 1	12	cm
$\overline{h_2}$	Liquid level in Tank 2	12	cm
$\bar{T}_i$	Feed liquid temperature	29	^oC
$\bar{T}_1$	Liquid temperature in Tank 1	29.9	^oC
$\overline{T_2}$	Liquid temperature in Tank 2	29.9	^oC
$\bar{q}$	Steady-state heat input	330	watt
ρ	Fluid density (water)	1.00	g/cm^3
Cp	Heat capacity	4,2	J/gr^{o}C
A_1, A_2	Area of tanks	346.36	cm^2
C_{V1}	Valve coefficient for Tank 1	25,90	-
C_{V2}	Valve coefficient for Tank 2	25,90	-

Table 2. Transfer Function Parameters

Symbol	Description	Value	Unit
K_{p1}	Mass process gain	0.2657	sec/cm^3
K_{p2}	Volumetric Thermal process gain (for flow rate)	-0.01	^{o}C.sec/cm^3
K_{p3}	Thermal process gain (for inlet temp)	1	cm^3/sec
K_{p4}	Thermal process gain (for heat input)	0.0027	^{o}C.sec/J
K_{p5}	Thermal process gain (for path 2 flow)	-0.01	^{o}C.sec/cm^3
τ_{p1}	Mass process time constant	92.65	sec
τ_{p2}	Thermal process time constant 1	46.32	sec
τ_{p3}	Thermal process time constant 2	46.32	sec
ξ_1	Damping factor for mass response	1	
ξ_2	Damping factor for thermal response 1	1	
ξ_3	Damping factor for thermal response 2	1	

Model validation was performed by comparing the response of laboratory experimental data to numerical model simulations (Explicit Euler) and analytical solutions (Laplace Invert) (Kim & Parovik, 2022). The test was conducted using step disturbances in the feed flow rate (fi). To quantitatively evaluate the accuracy and goodness-of-fit of the models, statistical metrics including the Coefficient of Determination (R^2), Root Mean Square Error (RMSE), and Mean Absolute Percentage Error (MAPE) were employed.

4.1 Step Decrease fi

The value of variable fi decreases abruptly according to the step decrease function from its steady state of 89.73 cm^3/sec to 57.75 cm^3/sec. Meanwhile, the other variables remain at their respective steady states. The data from the step decrease disturbance fi experiment and its mathematical modeling can be seen in Figure.5.

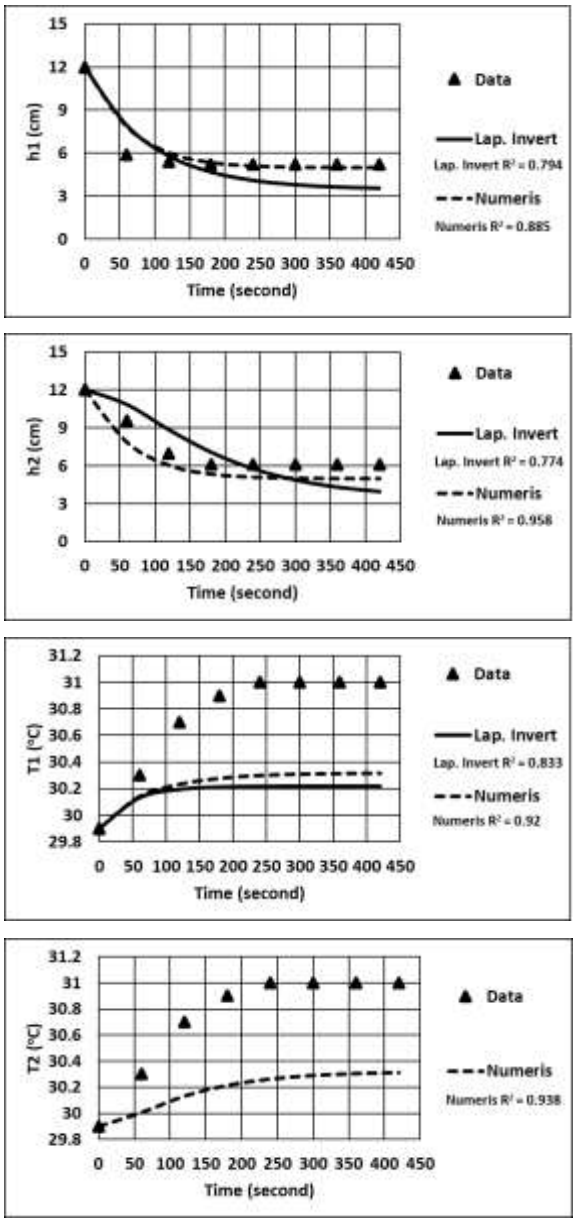

Figure. 5. Dynamic response to step decreases fi 35%

As shown in Figure. 5, when the feed flow rate was decreased by 35% from 89.73 to 57.75 cm³/sec, the liquid levels in Tank 1 (h_1) and Tank 2 (h_2) decreased exponentially toward a new equilibrium point. The temperature response shows an inverse correlation. A decrease in flow rate causes an increase in temperature because the ratio of heating energy to liquid mass increases.

4.2 Step Increase fi

The value of variable fi is suddenly increased according to the step increase function from its steady state of 89.73 cm^3/sec to 136.5 cm^3/sec. Meanwhile, the other variables remain at their respective steady states. The data from the step increase disturbance fi experiment and its mathematical modeling can be seen in Figure. 6.

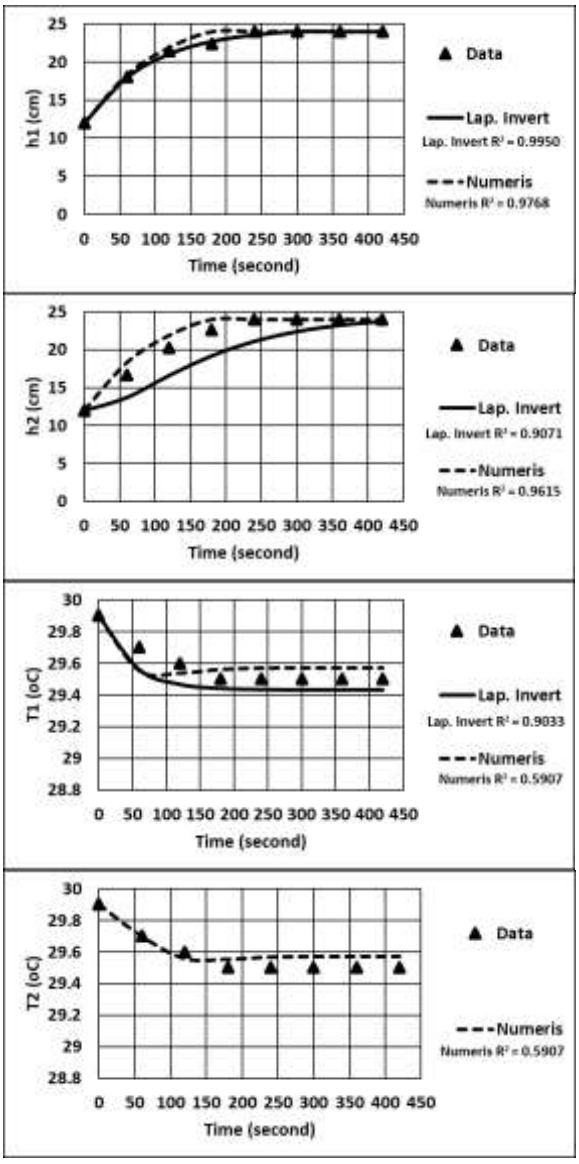

Figure. 6. Dynamic response to step increase fi 52%

An increase in the feed flow rate (f_i) triggers a rise in the liquid level of Tank 1 (h_1). This phenomenon is driven by mass accumulation, where the fluid inflow rate exceeds the outflow rate from the tank. Based on the experimental results, under an extreme step increase disturbance of 52%, h_1 surged rapidly, exceeding the tank's capacity limit (overflow). Similar dynamics were observed in the liquid level of Tank 2 h_2, which is directly influenced by Tank 1. The rise in h_1 drives an increase in the inter-tank flow rate f_1, leading to fluid mass accumulation in Tank 2, consequently causing h_2 to also reach an overflow state under the 52% step increase.

Conversely, the thermal response dynamics exhibit an inverse relationship compared to the hydraulic response. An increase in the feed flow rate f_i directly results in a temperature drop in Tank 1 T_1. This temperature decrease occurs because the additional fluid mass in the tank is not compensated

by an increase in heating power q_e. The heater operates at a constant rate, resulting in lower heat energy provided per unit mass. This cooling effect propagates sequentially to Tank 2 T_2. The fluid with a lower outlet temperature from Tank 1 enters Tank 2, causing T_2 to concurrently experience a gradual decline until a new steady-state condition is achieved.

In general, the results of the mathematical model simulation were able to follow the experimental data trends very well, both for level and temperature responses. The slight deviation that occurs in the initial transient phase is caused by the linearization assumption in the model, whereas the physical system has non-linear characteristics in the valve and fluid dynamics. However, this model is declared valid for representing the dynamics of the system within the tested operational range.

4.3 Step Decrease q_e

The value of the q_e variable decreased abruptly according to the step decrease function from its steady state of 330 watts to 92.3 watts. Meanwhile, the other variables remained at their respective steady states. The data from the qe disturbance step decrease experiment and its mathematical modeling can be seen in Figure. 7.

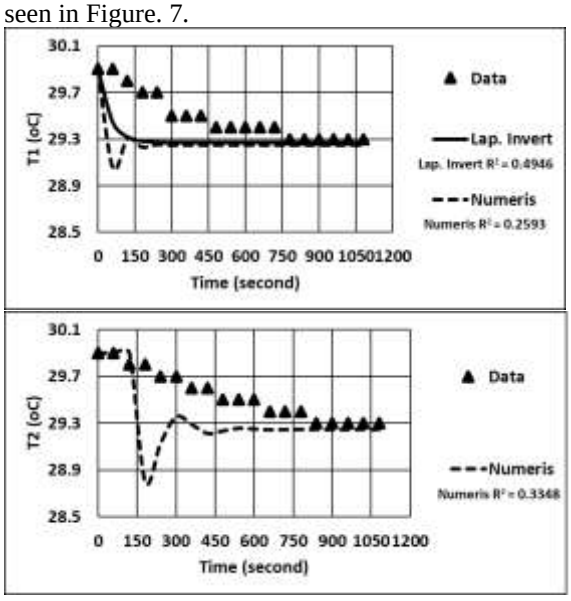

Figure. 7. Dynamic response to step decrease qe 72%

A reduction in the heating power q_e leads to a gradual decrease in the liquid temperature of Tank 1 T_1 until a new steady state is achieved. This thermal decline is attributed to the diminished heat input combined with the continuous influx of lower-temperature feed fluid, which effectively cools the liquid within Tank 1. Consequently, the temperature in Tank 2 T_2 exhibits a similar downward trend, eventually stabilizing at a new steady-state condition. This sequential cooling effect occurs because Tank 2 is directly fed by the effluent from Tank 1. Therefore, any temperature drops in the first tank, induced by the reduction in q_e, directly propagates to the second tank.

4.4 Step Increase qe

The value of the qe variable was suddenly increased according to the step increase function from its steady state of 330 watts to 559.35 watts. Meanwhile, the other variables remained at their respective steady states. The data from the qe disturbance step increase experiment and its mathematical modeling can be seen in Figure. 8.

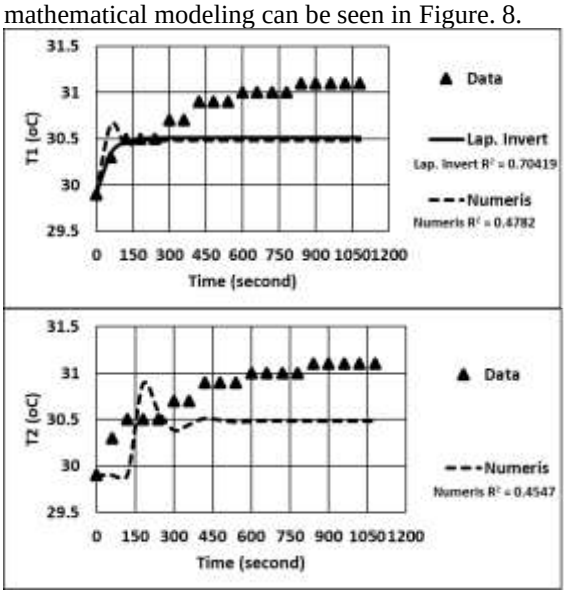

Figure. 8. Dynamic response to step increase qe 59.5%

An increase in the heating power q_e results in a proportional rise in the liquid temperature of Tank 1 T_1, which eventually stabilizes at a new steady-state condition. This temperature elevation is a direct consequence of the higher thermal energy supplied to the fluid within the tank. Subsequently, the temperature in Tank 2 T_2 exhibits a corresponding upward trend before reaching its own new steady state. This sequential heating effect occurs because Tank 2 is continuously fed by the effluent from Tank 1. Thus, the thermal surge induced by the elevated q_e in the primary tank directly propagates to the secondary tank.

To provide a comprehensive overview of the model's accuracy across all tested conditions, the statistical parameters (R^2, RMSE, and MAPE) for the dynamic profiles are summarized in Table 3.

Table 3. Statistical Evaluation of the Dynamic Models

Condition Variable	Model	R^2	RMSE/ MAPE
Step decrease f_i			
h_1	Analytical	0.794	1.274 cm/ 20.32%
	Numerical	0.885	0.765 cm/ 8.20%
h_2	Analytical	0.774	1.362 cm/ 17.78%
	Numerical	0.959	1.144 cm/ 15.17%

Condition Variable	Model	R^2	RMSE/ MAPE
T_1	Analytical	0.833	0.645 °C/ 1.89%
	Numerical	0.921	0.577 °C/ 1.70%
T_2	Numerical	0.938	0.616 °C/ 1.80%
Step increase f_i			
h_1	Analytical	0.995	0.255 cm/ 0.86%
	Numerical	0.977	0.645 cm/ 1.78%
h_2	Analytical	0.907	2.503 cm/ 10.63%
	Numerical	0.962	0.972 cm/ 3.28%
T_1	Analytical	0.903	0.092 °C/ 0.28%
	Numerical	0.591	0.079 °C/ 0.25%
T_2	Numerical	0.836	0.061 °C/ 0.18%
Step decrease qe			
T_1	Analytical	0.495	0.229 °C/ 0.56%
	Numerical	0.259	0.294 °C/ 0.70%
T_2	Numerical	0.335	0.315 °C/ 0.71%
Step increase qe			
T_1	Analytical	0.704	0.403 °C/ 1.06%
	Numerical	0.478	0.430 °C/ 1.17%
T_2	Numerical	0.455	0.463 °C/ 1.36%

4.5 Stability Analysis Using Nyquist Plot

Stability analysis is performed by plotting the open loop transfer function of the overall system on the Nyquist complex plane. The analysis is divided into two main reviews: hydraulic stability (fluid level) and thermal stability (temperature).

1) System Stability of Liquid Level

Based on the Nyquist plot for the overall mass balance (Figure. 9), the level system exhibits very high stability characteristics (robust). The response curve moves away from the critical point (-1, j0) across the entire frequency range. This indicates that the non-interacting series two-tank system has a large hydraulic damping capacity, so that disturbances in the inflow rate will not cause level instability as long as there is no overflow.

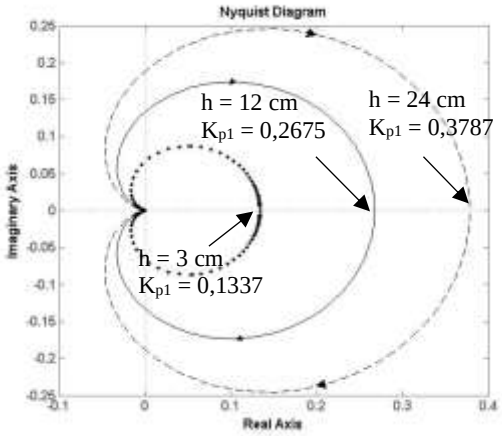

Figure. 9. Overall mass balance Nyquist plot

2) Thermal System Stability Limits (Heat Balance)

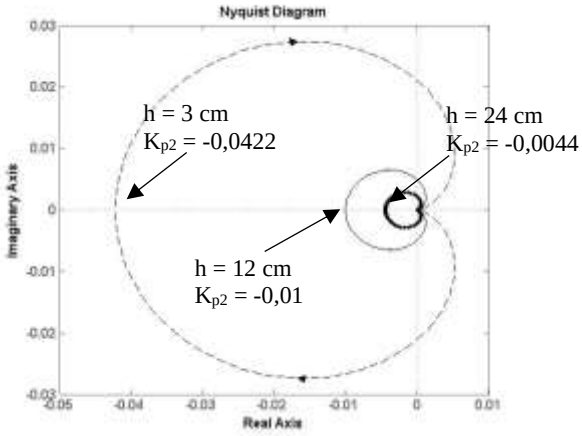

Figure. 10. Overall Heat Balance Nyquist Plot if q_e Steady

Based on Figure. 10, the open-loop Nyquist plot for the overall heat balance with f_i as the input and q_e steady demonstrates that the system is inherently stable across all operational levels (Ball, 1999), as none of the curves encircle or approach the critical point (-1, j0). However, the system's sensitivity to flow rate disturbances changes significantly depending on the liquid level. At a low level (h = 3 cm), the system exhibits the largest negative steady-state gain (K_{p2} = -0.0422), indicating high sensitivity where a small change in feed flow will drastically reduce the tank's temperature. Conversely, at a high level (h = 24 cm), the gain shrinks significantly (K_{p2} = -0.0044). This proves that a larger volume of water provides higher thermal inertia, dampening the reverse-acting effect of the incoming flow and making the temperature much more robust against flow rate fluctuations.

Figure. 11 illustrates the open-loop Nyquist plot for the overall heat balance of the system when the feed flow rate (f_i) is kept steady and the heater power (qe) is varied. The trajectories are located entirely on the positive real axis, confirming the direct-acting

nature of the heating process; an increase in heat input directly results in an increase in the tank's temperature. Furthermore, the plot clearly demonstrates the profound effect of thermal inertia associated with the liquid volume. At a low liquid level (h = 3 cm), the system exhibits the highest positive steady-state gain (K_{p4} = 0.0062), producing the largest Nyquist contour. This indicates maximum sensitivity, where a small change in heater power causes a significant and rapid temperature rise due to the small mass of water. Conversely, at the maximum operational level (h = 24 cm), the gain decreases substantially (K_{p4} = 0.0018), and the contour shrinks towards the origin. This proves that a larger water volume acts as a thermal buffer, dampening the temperature response and making the system more robust against heating variations. Finally, all trajectories smoothly approach the origin without encircling or nearing the critical point (-1, j0), verifying that the open-loop heating process is inherently stable across all volume capacities.

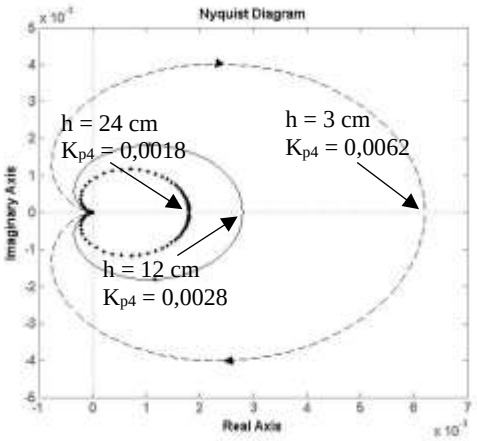

Figure. 11. Overall Heat Balance Nyquist Plot if f_i Steady

A rigorous evaluation of the plotted Nyquist trajectories in Figure. 9, Figure. 10, and Figure. 11 reveals distinct characteristics regarding the relative stability margins of the multi-capacity process. Because the open-loop frequency response profiles occupy locations exclusively isolated from the negative real axis and do not encircle or cross the critical threshold of (-1, j0), both the gain margin (GM) and phase margin (PM) for this system are theoretically infinite (∞). From a practical processing perspective, these boundless margins confirm that the open-loop thermal and hydraulic networks possess immense inherent resilience. The system can tolerate severe structural variations or sudden increases in processing gain without shifting toward unstable, oscillatory behavior, thereby ensuring a highly forgiving baseline for subsequent closed-loop automation.

5. Conclusion

This work successfully evaluated the transient responses and frequency-domain behavior of a non-interacting two-tank series thermal process. Both experimental and mathematical results confirm that the system is inherently stable and self-regulating in an open-loop conFigureuration. It could handle large, asymmetric load disturbances (+52% and -35%) while maintaining liquid heights between 3–24 cm and feed flows between 40.33–136.5 cm^3/s. From a control engineering perspective, Tank-01 follows typical first-order dynamics, whereas Tank-02 displays a clear overdamped second-order response with zero overshoot. In the frequency domain, the Nyquist criteria mathematically proved this absolute stability, yielding a maximum level gain of 0.3787 and a thermal process gain of 0.0062, combined with theoretically infinite (∞) gain and phase margins.

However, some limitations of this study should be noted. The mathematical analysis is built upon linearized lumped-parameter models, which might slightly underrepresent localized non-linear thermal behaviors during wider operating shifts. Additionally, the stability analysis was strictly limited to an open-loop setup, leaving out the practical behaviors caused by automated controller actions. Future studies should therefore focus on building high-fidelity non-linear dynamic models that eliminate quasi-static assumptions. Moreover, using the quantitative parameters and frequency baselines established here, subsequent work should introduce closed-loop control strategies—such as PID or Model Predictive Control (MPC)—to improve disturbance rejection and thermal efficiency in real industrial applications.

References

Akkoç, M. T. (2025). Fuzzy-PID Controller for Coupled Tank Systems. *Journal of Intelligent Decision Making and Granular Computing*, *1*(1), 256–265.

Ball, R. (1999). The origins and limits of thermal steady–state multiplicity in the continuous stirred tank reactor. *Proceedings of the Royal Society of London. Series A: Mathematical, Physical and Engineering Sciences*, *455*(1981), 141–161.

Ballesteros-Moncada, H., Herrera-López, E. J., & Anzurez-Marín, J. (2015). Fuzzy model-based observers for fault detection in CSTR. *ISA Transactions*, *59*, 325–333.

Borisov, M., Dimitrova, N., & Simeonov, I. (2020). Mathematical Modeling and Stability Analysis of a Two-Phase Biosystem. *Processes*, *8*, 791. https://doi.org/10.3390/pr8070791

Chen, S., Cao, X., Liu, Y., Wang, Z., & Zhang, J. (2024). Multi-frequency oscillation characteristics and stability of the pumped storage power station based on a theoretical analytical method. *Journal of Energy Storage*,

102, 114016. https://doi.org/https://doi.org/10.1016/j.est.2024.114016

Hermawan, Y. D., Reningtyas, R., Kholisoh, S. D., & Setyoningrum, T. M. (2016). Design of Level Control in A 10 L Pure Capacitive Tank: Stability Analysis and Dynamic Simulation. *International Journal of Science and Engineering*, *10*(1), 10–16.

Hermawan, Y. D., Yogi Suksmono, E. S., Cicilia, E., & Aisyiah, D. S. (2010). Dinamika Suhu pada Sistem Tangki-Seri-Tak-Berinteraksi dengan Arus Recycle. *Prosiding Seminar Nasional Teknik Kimia "Kejuangan" ISSN*, *1693*, 4393.

Kim, V. A., & Parovik, R. I. (2022). Application of the explicit Euler method for numerical analysis of a nonlinear fractional oscillation equation. *Fractal and Fractional*, *6*(5), 274.

Naik, R. B. B., & Kanagalakshmi, S. (2020). Mathematical modelling and controller design for interacting hybrid two tank system (IHTTS). *2020 Fourth International Conference on Inventive Systems and Control (ICISC)*, 297–303.

Nise, N. S. (2025). *Control Systems Engineering*. John Wiley & Sons, Limited. https://books.google.co.id/books?id=nFIrEQAAQBAJ

Ogata, K. (2020). *Modern control engineering*.

Seborg, D. E., Edgar, T. F., Mellichamp, D. A., & Doyle, F. J. (2016). *Process Dynamics and Control*. Wiley. https://books.google.co.id/books?id=ZZVFEAAAQBAJ

Suryatini, F., Salam, A., & Natasha, S. (2024). Water Level Control in Coupled Tank System with PLC and IoT-Based PID Method. *The Indonesian Journal of Computer Science*, *13*(4).

Tunjung, D., Prajitno, P., & Handoko, D. (2021). Temperature and water level control system in water thermal mixing process using adaptive fuzzy PID controller. *Journal of Physics: Conference Series*, *1816*(1), 12032.

Wang, Q., Chen, S., Chen, F., Zhang, J., Chen, L., Li, J., & Dou, Z. (2024). A dynamic assessment method for risk evolution in chemical processes based on MFM-HAZOP-FDBN. *Chemical Engineering Research and Design*, *204*, 471–486. https://doi.org/https://doi.org/10.1016/j.cherd.2024.02.049